RESEARCH ARTICLE

Solubility Enhancement of Palbociclib Supersaturable Self-Nano Emulsifying Drug Delivery System by Central Composite Design

Rajinikanth Chandran*, Kathiresan Krishnasamy

Department of Pharmacy, Annamalai University, Annamalai Nagar Chidambaram, Tamil Nadu, India.

Received: 12th January, 2024; Revised: 09th February, 2024; Accepted: 25th February, 2024; Available Online: 25th March, 2024

ABSTRACT

Nowadays, solid self-nano-emulsifying supersaturable drug delivery systems (S-SNEDDS) are being investigated to overcome the limitations of self-nano-emulsifying drug delivery systems (SNEDDS). The current study established S-SNEDDS for better drug dissolution and stability. S-SNEDDS were made with saturated solubility capryol® 90, labrosol®, and transcutol® HP. The composition was optimized using ternary phase diagrams. Palbociclib-SNEDDS created droplet size (Y1), polydispersity index (PDI) (Y2), and 15-minute drug release (Y3) responses using the central composite design (CCD) of response surface methodology (RSM). To optimise SNEDDS (S1) and evaluate S-SNEDDS, several precipitation inhibitors (PIs) were introduced. The best formulation, S1, had a minimum particle size of 129.34 nm and a maximum zeta potential (ZP) of 28.6 ± 2.12 mV. Unlike other inhibitors, methylcellulose kept the medicine supersaturated. The optimized formulation (F3) had a higher ZP (-24.6 ±1.8 mV) and smaller particle size (118.42 ± 1.26 nm), making it more stable than regular SNEDDS amorphous palbociclib was found in S-SNEDDS utilizing differential scanning calorimetry (DLS) and X-ray powder diffraction (PXRD). F3 released >99% in 90 minutes, compared to 19% for pure drug dispersion and 95% for SNEDDS. Results showed that S-SNEDDS formulation improved palbociclib solubility and stability.

Keywords: Palbociclib, Kinase inhibitor, Solubility, Droplet size, Polydispersity index, Drug release.

International Journal of Pharmaceutical Quality Assurance (2024); DOI: 10.25258/ijpqa.15.1.27

How to cite this article: Chandran R, Krishnasamy K. Solubility Enhancement of Palbociclib Supersaturable Self-Nano Emulsifying Drug Delivery System by Central Composite Design. International Journal of Pharmaceutical Quality Assurance. 2024;15(1):169-177.

Source of support: Nil.

Conflict of interest: None

INTRODUCTION

Palbociclib, an oral CDK inhibitor, may treat cancer. Palbociclib selectively inhibits CDK4 and CDK6, halting the cell cycle and preventing early G1 retinoblastoma protein phosphorylation. It slows tumor growth and DNA replication. Cell cycle regulators CDK4 and 6 are upregulated in many cancer cell types.[1] Oral capsule palbociclib (Ibrance) and letrozole were authorized as a breakthrough therapy for metastatic breast cancer in February 2015.[2]

Numerous clinical trials are testing palbociclib alone or in combination in various tumor cells with promising results.[3] Palbociclib fights human cancer cell lines, xenografts, and primary tumors.[4] Starting dose: 125 mg once a day for 21 days, seven days of therapy in a 28-day cycle, 2.5 mg letrozole continuously.[5] Palbociclib is a biopharmaceutics classification system (BCS) Class II non-hygroscopic crystalline powder.[6] Oral bioavailability (BA) is 46%, steadying after eight days with a median accumulation ratio of 2.4.[7]

Pharmacokinetic features, including poor absorption and diminished BA can induce inter- and intra-patient variations in drugs with pH-dependent solubility, notably basic substances. Thus, palbociclib needs new formulations to improve dissolution and BA. Solid dispersions, co-amorphous salts with organic acids, TPGS-PLA micelles, and chitosan-polypropylene glycol nano vehicles worked poorly for palbociclib distribution.[8] Lipid-based preparations were used to overcome these limits, and self-nano-emulsifying drug delivery systems (SNEDDS) have shown promising outcomes in the oral delivery of very lipophilic drugs due to their ease of production, realistic solubility increase, and oral BA.[9]

SNEDDS formulations of poorly soluble medicines can precipitate in gastric media, reducing solubility and BA.[10] Increasing surfactant was the usual solution. However, numerous surfactants in SNEDDS may cause gastrointestinal irritation and injury.[11] Solid-SNEDDS improves intestinal absorption of poorly soluble drugs. S-SNEDDS, a newer technique, prevents drug precipitation and creates meta-stable supersaturation with a hydrophilic polymeric PI. S-SNEDDS formulations increase poorly hydrophilic drug oral absorption BA.[12]

To our knowledge, lipid-based drug administration has not been explored to improve palbociclib BA. This study

*Author for Correspondence: rajinichan@gmail.com

produced S-SNEDDS for palbociclib to enhance oral BA. The ideal SNEDDS excipient composition was established using trial-and-error and univariate one-factor-at-a-time (OFAT) methods. The empirical trial-and-error method is instinctual, indiscriminate, and relies on the formulator's talent and knowledge, while the standard OFAT method adjusts one aspect at a time while maintaining all others. OFAT is expensive, time-consuming, and fails to estimate variable interactions. The OFAT method is inefficient and imprecise for determining the genuine 'optimum' due to several components' important interplay and quadratic influences. Response surface methodology (RSM) optimises manufacturing using statistics.[13]

Thus, statistical Design of Experiment (DoE) has become more prominent in design. DoE reliably calculates factor effects and interactions and speeds up optimization by grid searching the factor space with fewer exploratory runs. DoE requires fewer experimental trials and reveals synergistic effects or interactions between components, resulting in a robust formulation with economic time, money, and development benefits.[14] Most response surface experiments employ central composite design (CCDs). CCDs analyze curvature with axial (star) and center points in factorial or fractional factorial designs. CCD arrays have limited edge, center, and side factor levels. Central Composites fit quadratic models. These procedures are popular for sequential experimentation because they use data from a carefully constructed factorial trial.[15] This work used the DoEs to optimize palbociclib S-SNEDDS. CCD was used to assess formulation factors' main, interaction, and quadratic impacts on the size of the droplets, polydispersity index (PDI), and the total amount of the medication released after 15 minutes.

MATERIALS AND METHODS

Materials

Hyderabad-based Hetero Drugs Pvt. Ltd. provided palbociclib as a gift. Merck Life Science Private Limited (Hyderabad, India) supplied Capryol® 90, Caprylic and capric acid triglycerides (Labrafac Lipophile WL 1349 and Captex® 300), Mainsine®-35, Mauroglycol® 90, and Peceol®. Ethoxylated castor oil (Cremophor®-EL), hydrogenated castor oil (Cremophor® RH40), caprylocaproyl macrogol glycerides (Labrasol®), propylene glycol, ethanol, polyethylene glycols (PEG 400 and PEG 600), and diethylene glycol monoethyl ether were used. Mumbai-based Hi-media supplied DM-70 dialysis membrane (MWCO 10000). Other compounds were analytical-grade and used unpurified.

Table 1: List of IDV and DV in CCD

IDV			*Levels*			
Variable	*Name*	*Units*	*Low (-1)*	*High (+1)*	*-α*	*+ α*
A	Quantity of Capryol® 90	mg	30	40	26.59	43.40
B	Quantity of Labrasol®	mg	35	55	28.18	61.81
C	Quantity of Transcutol® HP	mg	15	25	11.59	28.40
DV			*Goal*			
Y_1	DLS	nm	Minimalize			
Y_2	PDI		Minimalize			
Y_3	DR after 15 min	%	Minimalize			

PDI, polydispersity index

Methods

Development of SNEDDS

- *Selection of formulation excipients*

The solubility saturation of palbociclib in various vehicles was analyzed using the preferred approach[16] to monitor the appropriate oil phase (OP), surfactant (SF), and co-surfactant (CSF). A precisely measured volume of supernatants was appropriately diluted using methanol, and the palbociclib concentration was assessed by UV (Shimadzu-1200) at 220 nm.

Construction of pseudo-ternary phase diagram

The three excipients represent the apex of the triangle that makes up the self-nano emulsifying zone that is assessed via ternary diagrams (using the XLSTAT add-on statistical programme).[17] The formulation excipients were combined and vortexed for 60 seconds to aid in homogenization. The formation of a nanoemulsion was tested by combining 100 mg with 25 mL of water and then agitating the mixture moderately. The compositions' visual appeal and ease of emulsification were assessed.

Compatibility study of drug-excipient

The drug's spectra and physical mixture (1:1) were recorded using Fourier-transform infrared spectroscopy (FTIR) with an FTIR Spectrophotometer that scanned between 4000 and 400 cm^{-1}. The apparatus used to record the differential scanning calorimetry (DSC) was Perkin Elmer DSC/7 DSC. A Hitachi S-3000 N with a hastening voltage of 10 Kv and a magnification of 5000X was used for the scanning electron microscope (SEM) examination.

DoE-CCD

To study and optimize the impacts of formulation excipients on SNEDDS, a 3^2CCD was utilized (Table 1). Stat-Ease Design Expert® software V8.0.1, which includes a CCD model, was used to run twenty model tests. Table 2 specifies the circumstances, and the results are tabulated. Individual response parameters were analysed using quadratic models with repeated linear regression analysis for each response parameter, as shown in Equation 1.

$$Y = \beta_0 + \beta_1 X_1 + \beta_2 X_2 + \beta_3 X_1 X_2 + \beta_4 X_1^2 + \beta_5 X_2^2 + \beta_6 X_1 X_2^2 + \beta_7 X_1^2 X_2 \quad (1)$$

Y -The magnitude of the measured response
β_0- intercept
β_1 - β_7- regression coefficients
X_1, X_2 - main effects
X_1, X_2 -interaction among X_1, X_2
X_1^2 and X_2^2- quadratic terms

Table 2: CCD with observed responses

Run	*Quantity of Capryol® 90 (mg)*	*Quantity of Labrasol® (mg)*	*Quantity of Transcutol® HP (mg)*	*DLS (nm)*	*PDI*	*DR after 15 minutes*
1	35	45	20	187.24	0.192	71.24
2	35	45	11.59	206.53	0.272	59.83
3	35	45	20	184.67	0.187	72.12
4	35	45	28.4	229.12	0.236	67.63
5	35	45	20	185.78	0.186	70.96
6	40	55	25	296.87	0.424	66.73
7	30	35	15	168.93	0.202	73.14
8	35	61.81	20	362.65	0.542	65.72
9	40	55	15	267.55	0.376	63.12
10	35	45	20	189.32	0.182	71.98
11	26.59	45	20	202.43	0.267	74.56
12	43.4	45	20	173.23	0.136	75.48
13	30	55	15	284.12	0.284	63.12
14	40	35	25	136.51	0.128	78.34
15	40	35	15	152.23	0.238	72.68
16	35	45	20	186.82	0.19	70.54
17	30	35	25	148.12	0.142	76.84
18	35	45	20	183.43	0.172	72.46
19	35	28.18	20	141.12	0.258	78.48
20	30	55	25	312.34	0.387	67.32

The plot was used to assess the impacts of A, B, and C on Y1 and Y2.[18] Derringer's desirability functionality was utilized to determine the best SNEDDS setup.

Selection of Precipitation Inhibitor

By combining various precipitation inhibitors (PIs) with the optimized SNEDDS formulation, several S-SNEDDS were created. At 37°C and 100 rotations per minute, 1000 mg of optimized palbociclib SNEDDS and PIs were combined with 100 mL of simulated gastric fluid (SGF) medium. About 1-mL of this solution was extracted at 5 to 240 minutes at fixed intervals, followed by 3 minutes of centrifugation. The liquid remaining after centrifugation was mixed with methanol, and the amount of palbociclib present was measured using a spectrophotometer.

Preparation of Palbociclib-loaded SNEDDS and S-SNEDDS Formulation

Palbociclib-loaded SNEDDS was created by dissolving it in OP, SF, and CSF. To achieve complete drug solubility, the components were swirled and vortexed at 37°C. S-SNEDDS formulation is accomplished by incorporating varying amounts of a specified precipitation inhibitor into an optimized SNEDDS formulation.[19]

Estimation of droplet size and ZP

Mastersizer 2000 (Malvern Instruments Ltd, UK) was utilized to calculate the DLS in combination with the particle sizing programme MAS OPTION. The ZP was measured with an extra electrode attached to the above-mentioned apparatus.

The SEM analysis

The drug and SNEDDS' exterior surface and cross-section were examined using a Hitachi S4100 SEM at 15 keV accelerating voltage. To enhance contrast, one drop of the diluted emulsion was applied to a film-coated copper grid, which was then dyed with one drop of 2% (w/v) aqueous phosphotungstic acid before drying. SEM was used to analyze samples at 72000 magnifications.

Thermodynamic stability study

This was evaluated after six chilling (4°C) and heating (40°C) cycles and 48 hours of freeze-thaw (-21 & 25°C). The stable formulation was centrifuged at 3500 rpm for 30 minutes to test phase separation.[20]

Physicochemical characterization

The formulated SNEDDS and S-SNEDDS were analyzed using FTIR, DSC, PXRD, and SEM.

In-vitro dissolution study

The investigations used a 50-rpm USP type II device (Electrolab, TD L8, India). Palbociclib samples containing 10 mg were combined with 0.9 L of pH 6.8 buffer solution comprising 0.5% Tween 80 at 37 °C. At present time slots, 5 mL samples were withdrawn and replaced with a proportionate fresh medium. The contents were filtered, diluted, and drug-tested. Triplicate measurements were obtained.[21]

Kinetic analysis

Multiple release kinetic models were run on *in-vitro* dissolution data[22] to determine release order and mechanism.

Accelerated stability study

Samples were held for 3 months in a stability chamber at 40°C and 75% RH before being tested to verify the formulation's stability per ICH recommendations Q1A (R2).[23]

RESULTS AND DISCUSSION

Solubility Study

The highest drug solubility was found in capryol® 90, labrosol®, and transcutol® HP, which were used as excipients (Figure 1).

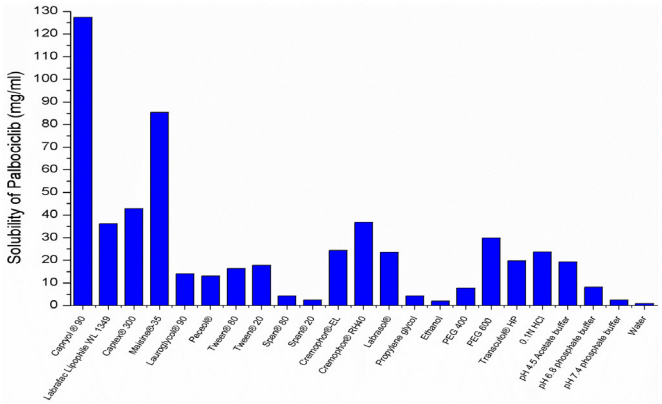

Each value represents the mean ± SD (n = 3)

Figure 1: Solubility of palbociclib in various vehicles

Selection of Oil, Surfactant, and Co-surfactant

This investigation chose SNEDDS oil based on its ability to solubilize most medications. Each surfactant's amount of oil emulsified was used to measure its emulsification capacity. Because of their polarity, co-surfactants should be used sparingly to improve pharmaceutical solubilization. Following aqueous dispersion, co-surfactants move to the water phase, resulting in medicament precipitation.[24]

Ternary Phase Diagram

For palbociclib SNEDDS preparation, capryol® 90 (oily phase), labrasol® (surfactant), and transcutol® HP (cosurfactant) were chosen based on solubility and emulsification tests. Figure 2 shows a pseudo-ternary phase diagram that found an emulsification area to optimize the formulations. Nano-emulsification occurs when aqueous dispersion produces homogenous, transparent systems. They found that raising the surfactant-to-cosurfactant ratio enhanced the area of the preparation due to the adsorption of surfactants at the emulsion interface, which decreased surface tension and preparation DLSs. The drug ingredients in SNEDDS affect their performance. In the presence of palbociclib, a ternary phase diagram was constructed. Due to palbociclib's low water solubility, drug molecules may orient at nanoemulsion interfaces. The green region represents the efficient self-nanoemulsifying region in Figure 2. According to the picture, component ranges were chosen: Capryol®90 ≤ 40%, Labrasol® ≤ 54%, and Transcutol® HP ≤ 25%.

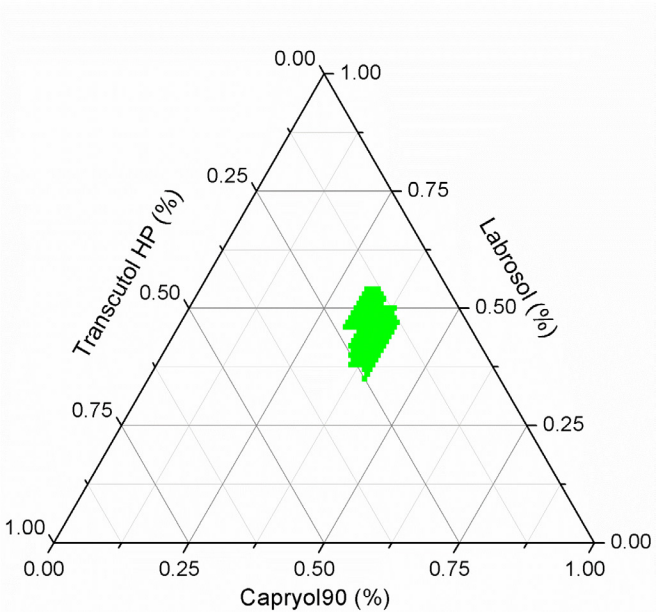

Figure 2: Ternary phase diagram of palbociclib loaded SNEDDS

Drug and Excipients Compatibility Study

To identify the drug and excipients and determine their interaction, FTIR and DSC absorption spectra of pure drug, all chosen excipients, and the physical combination were collected. IR spectra of palbociclib, capryol® 90, labrasol®, transcutol HP. The physical composition showed large distinctive peaks (Figure 3). The drug's principal characteristic peaks were at the same wave numbers, indicating no chemical interactions with the specified adjuvants. Physical mixing resulted in the discovery of some new peaks, possibly due to excipient functional groups.

Figure 3 shows a clear symmetric endothermic peak at 276.55°C, pure palbociclib's melting point. The capryol® 90 DSC curve displays an enothermic peak at 107.1°C. The DSC of labrasol® shows an endothermic peak at 310.49°C. The DSC of transcutol HP shows an endothermic peak at 116.92°C. The DSC of the physical blend shows 2 endothermic transcutol HP and palbociclib peaks. The DSC of the physical blend showed the drug's obvious endothermic peak, indicating no chemical interactions with the specified excipients.

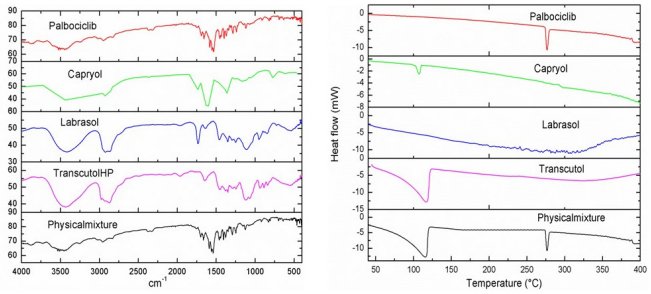

Figure 3: FTIR & DSC spectrum of palbociclib, capryol® 90, labrasol®, transcutol® HP, and physical mixture

Design Summary

File Version	8.0.1.0		
Study Type	Response Surface	Runs	20
Design Type	Central Composite	Blocks	No Blocks
Design Model	Quadratic	Build Time (ms)	7.47

Factor	Name	Units	Type	Subtype	Minimum	Maximum	-1 Actual	+1 Actual	Mean	Std. Dev
A	Amount of capryol 90	mg	Numeric	Continuous	26.59	43.41	30.00	40.00	35.00	4.13
B	Amount of Labrasol	mg	Numeric	Continuous	28.18	61.82	35.00	55.00	45.00	8.26
C	Amount of transcutol HP	mg	Numeric	Continuous	11.59	28.41	15.00	25.00	20.00	4.13

Response	Name	Units	Obs	Analysis	Minimum	Maximum	Mean	Std. Dev.	Ratio	Trans	Model
Y1	Droplet size	nm	20	Polynomial	136	362	209.5	62.5001	2.66176	None	RQuadratic
Y2	PDI		20	Polynomial	0.128	0.542	0.25005	0.107631	4.23438	None	RQuadratic
Y3	Drug release after 15mir	%	20	Polynomial	59.83	78.48	70.6145	5.159	1.31172	None	RQuadratic

Figure 4: The summary of CCD

DoEs

About 20 trials were based on CCD experimental runs. The DLS (Y1) was 136 to 362 nm, the PDI (Y2) was 0.128–0.542, and the 15-minutes drug release range (Y3) was 59.83 to 78.48%. (Figure 4). Substituting the responses into the quadratic model was found to have a non-significant lack of fit ($p > 0.1$), validating model fit. The 2nd order quadratic model (R^2) analysis of multiple regression measures variation near the mean.[25]

A F-value of 1126.09 indicates that the DLS (Y1) mathematical model is significant. A large "Model F-Value" owing to noise is 0.01% likely. "Prob > F" values below 0.0500 suggest important model terms. A, B, C, BC, B2, and C2

largely impact DLS. Values over 0.1000 imply insignificant model terms. The significant model terms that have *p-values* below 0.0500. The "Lack of Fit F-value" of 3.19 indicates that the sheer mistake outweighs the Lack of Fit. A "Lack of Fit F-value" this large is 10.83% likely attributable to noise. The model should fit; therefore, a non-significant lack of fit is good. According to the equation, B has a greater impact than A and C. DLS factorial equation correlated well (0.9981). Perturbation, contour, and 3D RSM plots revealed the main and interrelating impacts of independent variables (IDV) on DLS. See Figure 5 for the primary effects of A, B and C on DLS (Y1). The image shows that B has the greatest influence on Y1, followed by A and C. Three-dimensional RSM plots and contor plots illuminated the dependent-independent relationship. Figure 5 depicts B and C's effect on DLS at a fixed A. Figure 5 also depicts the contour plot. At low A levels, Y1 dropped from 312.34 to 148.12 nm. At high A levels, Y1 dropped from 296.87 to 136.51 nm. At low B levels, Y1 dropped from 168.93 to 136.51 nm. At high B levels, Y1 dropped from 312.34 to 267.55 nm. Y1 dropped from 284.12 to 152.23 nm at low C. Similarly, high C levels dropped Y1 from 312.34 to 136.51 nm. According to numerous SNEDDS articles, increasing surfactants (B) or decreasing oil (A) increases DLS and vice-versa. Higher surfactant concentrations with lesser oil amounts may form a thick coating on oil droplets, stabilising them.

Table 2 shows that the prepared SNEDDS had a PDI of 0.192 to 0.542. The quadratic model showed that labrasol® and transcutol® HP affect the PDI. Table 3 demonstrates the similarity between theoretical and observed values. The F-value of 35.07 indicates that the PDI (Y2) mathematical model is significant. A "Model F-Value" this large is just 0.01% likely due to noise. Model terms are significant if "Prob > F" is less than 0.0500. Model terms with "Prob > F" larger than 0.1000 are not significant. The "Lack of Fit F-value" of 34.64 indicates a major issue. Noise is just 0.06% likely to cause a significant "Lack of Fit F-value". An inadequate fit is undesirable; the model should suit properly. B has a greater influence than C, according to the equation. The PDI factorial equation correlated well (0.9261). The 3D RSM plots, perturbation, and contour plots provided insights into the principal and interdependent influences of factors on the PDI. Figure 6 The perturbation plot showing B and Con's main effects on Y2 polydispersity. This chart shows that B has more influence on Y2, followed by C's minimal impact. The relationship between the dependent variables (DV) and IDV was clarified using 3D RSM and contour plots. The figure shows B and C's PDI interaction at a fixed A level. Y2 fell from 0.387 to 0.142 at low A levels. Likewise, high A levels reduced Y2 from 0.424 to 0.128. Y2 fell from 0.238 to 0.128 at low B levels. Y2 fell from 0.424 to 0.284 at high B levels. At low temperatures, Y2 fell from 0.376 to 0.202. At high temperatures, Y2 decreased from 0.424 to 0.142.

Table 2 shows that SNEDDS formulations released 59.83–78.48% of their medication in 15 minutes. The quadratic model showed that capryol®90, labrasol®, and transcutol® HP affect 15-minutes drug release. The F-value for the mathematical

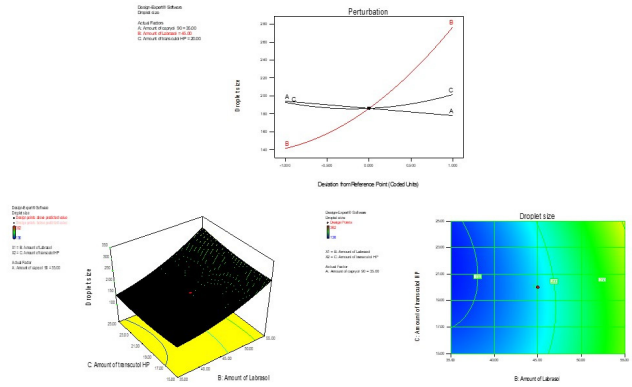

Figure 5: The perturbation, 3D RSM, and counterplots display the influence of formulation parameters on DLS

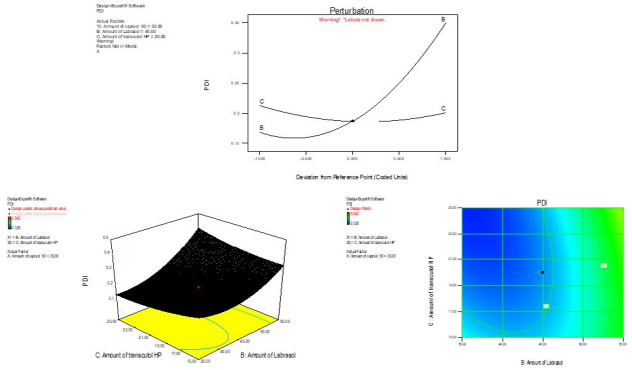

Figure 6: The perturbation, 3D RSM, and counterplots display the influence of formulation excipients on PDI

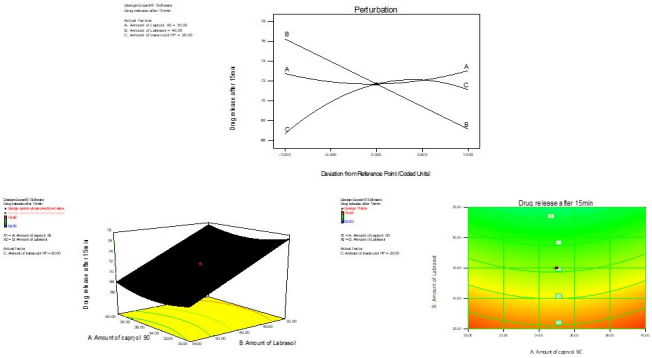

Figure 7: The 3D RSM and counterplot display the influence of formulation excipients on the percent drug release

model for %DR in 15 minutes (Y3) was 128.36, suggesting significance. A "Model F-Value" this large is just 0.01% likely due to noise. Model terms are noteworthy if "Prob > F" is less than 0.0500. Model terms above 0.1000 are insignificant. Its "Lack of Fit F-value" of 1.58 shows that it is not important compared to pure error. The risk of a large "Lack of Fit F-value" being caused by noise is 31.84%. A non-significant misfit is acceptable; the model should suit. According to the equation, B has a greater influence than A and C. The factorial equation for %drug release correlated well (0.9787). The 3D

Table 3: Regression equations for the responses – DLS, PDI, and %DR after 15 minutes

Response	*Regression equation*
Y_1	186.13 - 8.04 A + 67.85 B + 4.37 C + 11.62 BC + 23.12B^2+ 11.10 C^2
Y_2	0.19 + 0.091 B – 0.0058 C + 0.040 BC +0.072 B^2+ 0.020 C^2
Y_3	71.70 + 0.15 A – 4.55 B + 2.22 C + 1.2 A^2 – 2.79 C^2

RSM plots, perturbation, and contour, unveiled the principal and interdependent effects of distinct variables on the size of particles. The perturbation diagram in Figure 7 depicts the principal effects of A, B, and C on drug release (Y3). This chart shows that B influences Y3 the most, followed by C&A. C decreasing medication release at greater values. 3D RSM and contour graphs were employed to elucidate the correlation between the IDV and DV. The impact of A and B on the percent drug release at a constant C is illustrated in Figure 7. The figure also shows the contour plot. At low A levels, Y3 rose from 55.59 to 79.22%. At high amounts of A, Y3 rose from 54.28 to 81.92%. At low B, Y3 increased from 54.28 to 65.61%. As B levels increased, Y3 soared from 61.32 to 77.48%. At low C, Y3 increased from 63.61 to 81.92%. Likewise, elevated C concentrations increased Y3 from 60.9 to 79.22%.

Optimization by Desirability Function

The replies were converted into a desirability scale, with Y1 and Y2 being the least desirable and Y3 being the most desirable. The greatest function value was attained at A: 40, B: 35, and C: 22.91 (w/w) with the associated D value of 0.974. Three batches of SNEDDS under ideal conditions were designed to validate prediction adequacy, and replies were evaluated (Table 4). The model was deemed viable since there was a strong correlation between anticipated and observed values.

Evaluation of SNEDDS

The diluted palbociclib -SNEDDS DLS, PDI, and ZP were measured. The PDI of optimized SNEDDS was determined after a 100-fold dilution in distilled water. The optimized SNEDDS DLS and PDI were 129.34 to 134.86 nm and 0.146 to 0.168, respectively. The optimized SNEDDS ZP ranged from -25.9 ± 1.13 to -28.6 ± 2.12 mV. For formulation into S-SNEDDS, the formulation S1 with the smallest particle size was considered.

Screening of PI

Because S-SNEDDS are designed to surrender to a supersaturated state, the drug concentration and degree of supersaturation must be measured over time. Polymers

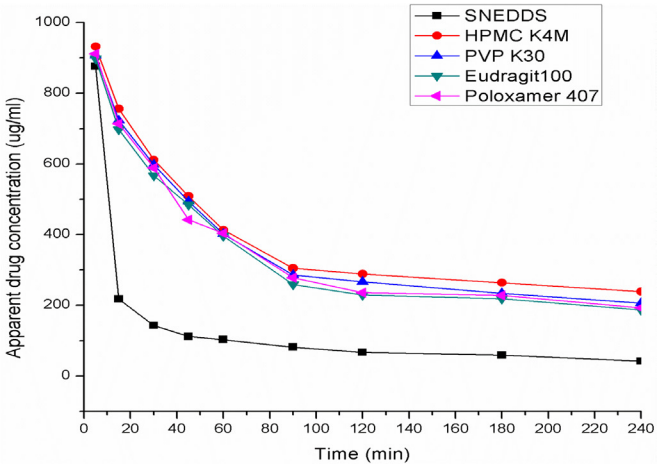

Figure 8: *In-vitro* mean apparent palbociclib concentration-time profiles observed from various polymer PIs

like HPMC K4M, PVP K30, Poloxamer 407, and Eudragit L100 were added to the optimised SNEDDS (S1) to generate S-SNEDDS.[26] Based on the experimental design, formulation S1 with the lowest DLS and highest ZP was chosen for formulation into S-SNEDDS. The precipitation profile revealed that S-SNEDDS were more resistant to drug precipitation than SNEDDS within 240 minutes. By employing the 100 dilution factor (10 mg palbociclib in 100 mL medium), it was possible to determine the concentration of palbociclib in the test medium to be 1000 µg/mL.

Palbociclib in SNEDDS was lowered to 218 µg/mL at t = 15 minutes and quickly to 143 µg/mL after 30 minutes owing to drug precipitation. In contrast, the S-SNEDDS preparation reliably outperformed the SNEDDS formulation in terms of palbociclib concentration-time profile. According to the findings, HPMC might more efficiently preserve the medication in a supersaturated form than other inhibitors (Figure 8).

A sequence of palbociclib S-SNEDDS was generated using varied quantities of HPMC to determine the influence of HPMC K4M on supersaturation states. The findings indicated that the precipitation inhibition outcome was enhanced as the concentration of HPMC K4M increased. No significant difference existed in the effectiveness of HPMC K4M between 2.0 and 5.0%. All formulations had a 1-minute emulsification time, indicating increased self-emulsification effectiveness. As a result, 2% HPMC K4M (F3) was chosen for future research.

The DLS and ZP of S-SNEDDS

The DLS of S-SNEDDS (F1-F4) was 118 to 128 nm with PDI 0.112 to 0.204, which is somewhat less than SNEDDS

Table 4: Optimized values obtained by the constraints apply on Y_1, Y_2, and Y_3

IDV	*Nominal values (mg)*	*Predicted values*			*Observed values*				
		DLS (Y_1) (nm)	*PDI (Y_2)*	*%DR in 15 min (Y_3)*	*Batch*	*DLS (Y1) (nm)*	*PDI (Y2)*	*%DR in 15 min (Y3)*	*ZP (mV)*
Quantity of capryol® 90 (A)	40				S1	129.34	0.168	76.32	-28.6 ± 2.12
Quantity of labrasol® (B)	35	132.90	0.148	77.94	S2	134.86	0.146	78.56	-25.9 ± 1.13
Quantity of transcutol® HP (C)	22.91				S3	132.32	0.152	75.88	-26.3 ± 2.98

Table 5: The DLS, PDI, and ZP of S-SNEDDS formulations

Sample	*DLS ± SD (nm)*	*PDI*	*ZP (mV)*
F1	128.34 ± 0.63	0.182±0.005	-23.9 ±1.4
F2	124.23 ± 2.12	0.197±0.005	-24.4 ±1.2
F3	118.42 ± 1.26	0.112±0.005	-24.6 ±1.8
F4	121.45 ± 1.34	0.204±0.005	-21.5 ±2.2

(Each experiment was conducted in triplicate, and the results were reported as means±standard deviations., n = 3)

(131–254 nm) owing to the incorporation of HPMC, which generated a physical barrier that surrounds the oil droplets, inhibiting aggregation and resulting in a lower size nano-emulsion (Table 5).

Thermodynamic Stability

After dispersion in water, the S-SNEDDS formulation (F3) produced a translucent emulsion that was examined at various temperatures and stress levels. The proposed formulation passed the thermodynamic stability test with no phase separation or precipitation across alternative temperature cycles (4 and 40°C), freeze-thaw cycles (-21 and +25°C), and centrifugation at 3500.

Physicochemical Characterization of Palbociclib S-SNEDDS

Figure 9 shows the physicochemical characterization of palbociclib S-SNEDDS. FTIR spectroscopy was utilized to assess the interaction between palbociclib and PI. Palbociclib's peak at 2997.47 cm^{-1} changed to 3082.35 cm^{-1} in S-SNEDDS. The peaks of palbociclib in the S-SNEDDS XRPD pattern were dull or eliminated, indicating a decrease in the crystalline structure of palbociclib. Palbociclib and S-SNEDDS exhibited sharp endothermic peaks at 276.5 and 288.4°C, respectively, corresponding to the drug's melting point. The S-SNEDDS showed no distinctive peak between 40 and 400°C, confirming the drug's amorphous nature.

SEM analysis indicated that the SNEDDS and S-SNEDDS are spherical in form and size (Figure 10).

In-vitro Dissolution Results

The S-SNEDDS dissolution profile reveals quicker drug release (43.5 ± 1.8% in 5 minutes) compared to pure drug dispersion and SNEDDS formulation (Figure 11). Self-emulsifying systems' low surface free energy may encourage rapid drug dissolution from S-SNEDDS by quickly establishing the interface between dissolution media and oil. The increased

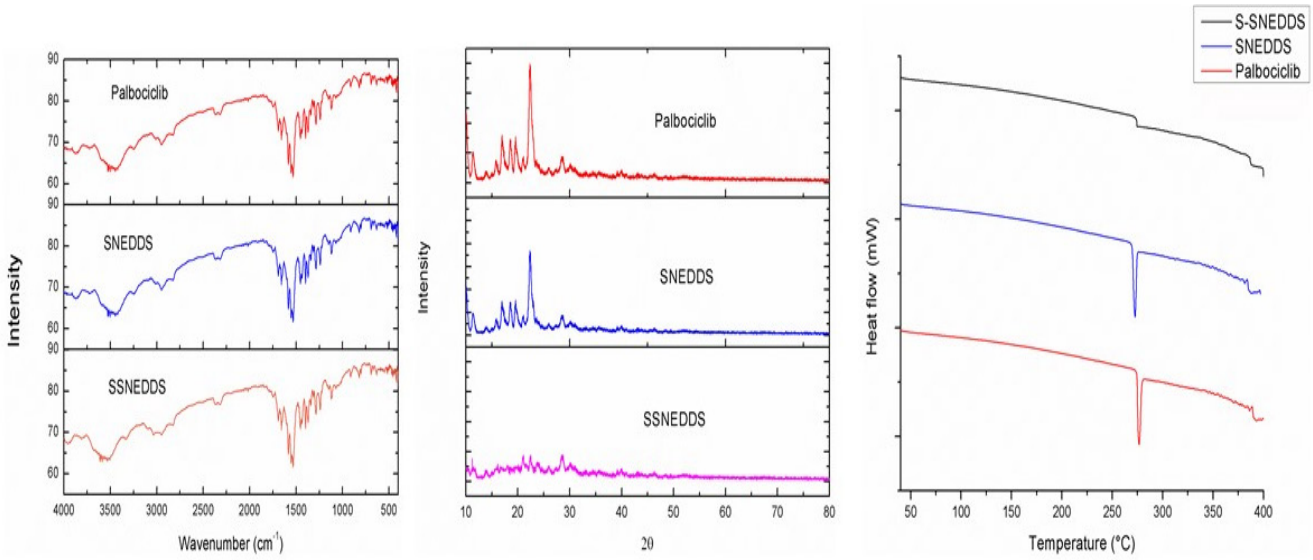

Figure 9: FTIR, XRPD & DSC spectra of pure palbociclib, drug loaded SNEDDS and S-SNEDDS

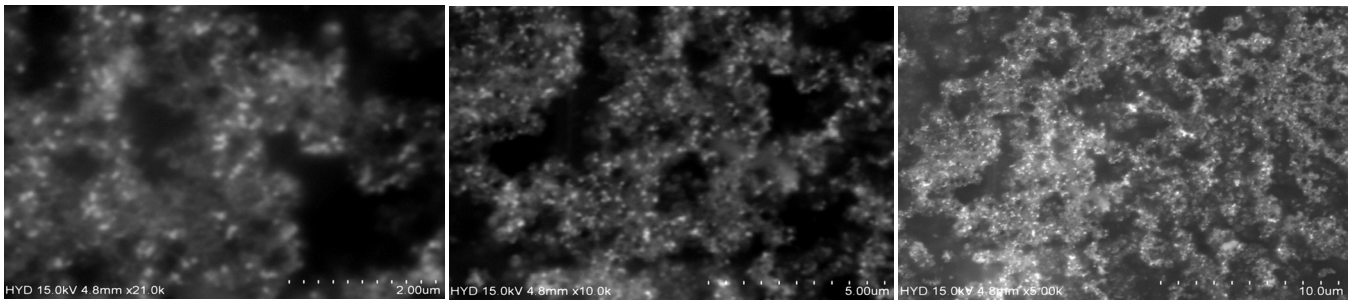

Figure 10: SEM images of palbociclib loaded S-SNEDDS formulation (F3)

Table 6: Release kinetics of optimized formulation of palbociclib SNEDDS

Formulation Code	*Zero order*		*First order*		*Higuchi*		*Korsmeyer-Peppas*	
	R^2	*n*	R^2	*n*	R^2	*n*	R^2	*n*
F3	0.48652	0.835	0.94188	-0.0262	0.7869	10.142	0.8746	44.81

Table 7: DLS, ZP, and PDI of palbociclib S-SNEDDS formulation following 90 days of refrigeration and room temperature storage

Temperature (°C)	*DLS (nm)*		*ZP*		*PDI*	
	0 months	*3 months*	*0 months*	*3 months*	*0 months*	*3 months*
4 ± 1°C	128.34 ± 0.63	131.78 ± 1.12	-23.83 ±1.4	-22.56 ± 2.2	0.182 ± 0.005	0.211 ± 0.005
25 ± 2°C	128.34 ± 0.63	132.56 ± 0.92	-23.83 ±1.4	-19.72 ±1.7	0.182 ± 0.005	0.196 ± 0.005

n = 3 ($p < 0.05$).

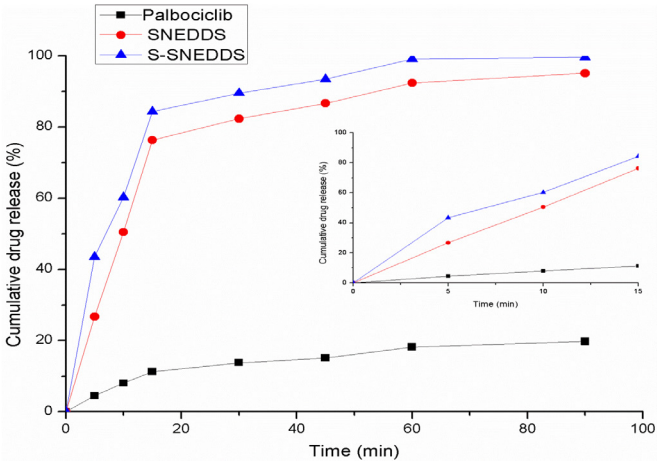

Figure 11: Dissolution profile of palbociclib from SNEDDS formulations

surface area of nanosized globules, as well as the transition of palbociclib from a low water-soluble crystalline form to a non-crystalline amorphous or disordered crystalline phase of molecular dispersion in S-SNEDDS, promotes dissolution.

Release Kinetics

The findings indicate that the regression coefficient value for the optimized formulation with n = 44.81 in first-order kinetics is close to 1. This is confirmed by the Korsmeyer-Peppas plots. The drug was administered through the super case II transport mechanism. The data on drug release kinetics are presented in Table 6.

Stability Study

Stability testing shows how the quality of medicine substances or products changes over time due to environmental conditions, including humidity, temperature, and light. Table 7 indicates no significant change ($p < 0.05$) in DLS, ZP, and PDI of optimized formulation at refrigerated and room temperature.

CONCLUSION

Capryol® 90, labrosol®, and transcutol® HP effectively formulated palbociclib-SNEDDS with a faster self-emulsifying time, excellent DLS, and ZP. About 20 investigations were conducted following the experimental runs and analyzed using Design-Expert software. The optimized formulation (S1) chosen from ternary phase diagram and CCD composed of capryol® 90: 40%, cremophor®-EL: 35% and transcutol® HP: 22.91% (w/w) was further incorporated with HPMC to convert to supersaturable SNEDDS which displayed rapidly *in-vitro* drug dissolution of over 99% in 90 minutes which is superior to that of SNEDDS(S1) release of 95% and pure drug dissolution of 19%. Better dissolution may be connected to nanosized globules' increased surface area and palbociclib's shift from crystalline to amorphous state. The stable supersaturate formulation exhibited better emulsifier ability and provided a constructive oral solid dosage form for poorly water-soluble medicines.

ACKNOWLEDGEMENT

The authors express their gratitude to the Management and Department of Pharmacy at Annamalai University, located in Annamalai Nagar, Chidambaram, Tamil Nadu, India, for their provision of research facilities. The authors express their gratitude to the Department Head and Principal of Pharmaceutical Sciences at Omega College of Pharmacy Edulabad, Hyderabad, Telangana, India for their valuable support and guidance.

REFERENCES

1. Niu Y, Xu J, Sun T. Cyclin-Dependent Kinases 4/6 Inhibitors in Breast Cancer: Current Status, Resistance, and Combination Strategies. Journal of Cancer 2019; 10(22):5504-5517.
2. Choi YJ, Anders L. Signaling through cyclin D-dependent kinases. Oncogene 2014; 33(15):1890–1903.
3. Chen F, Liu C, Zhang J, Xu W, Zhang Y. Progress of CDK 4/6 inhibitor palbociclib in the treatment of cancer. Anticancer Agents in Medicinal Chemistry 2018; 18(9):1241-1251.
4. Comstock CES, Augello MA, Goodwin JF, Leeuw RD, Schiewer MJ, Ostrander Jr WF, Burkhart RA, McClendon AK, McCue PA, Trabulsi EJ, Lallas CD, Gomella LG, Centenera MM, Brody JR, Butler LM, Tilley WD, Knudsen KE. Targeting cell cycle and hormone receptor pathways in cancer. Oncogene 2013; 32(48):5481–5491.
5. McShane TM, Wolfe TA, Ryan JC. Updates on managing advanced breast cancer with palbociclib combination therapy. Therapeutic Advances in Medical Oncology 2018; 10:1758835918793849.
6. Ruiz-Garcia A, Plotka A, O'Gorman M, Wang DD. Effect of food on the bioavailability of palbociclib. Cancer Chemotherapy and Pharmacology 2017; 79(3):527-533.

7. Luca A, Maiello MR, D'Alessio A, Frezzetti D, Gallo M, Carotenuto M, Normanno N. Pharmacokinetic drug evaluation of palbociclib for the treatment of breast cancer. Expert Opinion on Drug Metabolism and Toxicology 2018; 14(9):891-900.
8. de Melo-Diogo D, Gaspar VM, Costa EC, Moreira AF, Oppolzer D, Gallardo E, Correia IJ. Combinatorial delivery of Crizotinib-Palbociclib-Sildenafil using TPGS-PLA micelles for improved cancer treatment. European Journal of Pharmaceutics and Biopharmaceutics 2014; 88(3):718-729.
9. Inugala S, Eedara BB, Sunkavalli S, Dhurke R, Kandadi P, Jukanti R, Bandari S. Solid self-nano emulsifying drug delivery system (S-SNEDDS) of darunavir for improved dissolution and oral bioavailability: *In vitro* and *In vivo* evaluation. European Journal of Pharmaceutical Sciences 2015; 74:1-10.
10. Bevernage J, Brouwers J, Annaert P, Augustijns P. Drug precipitation-permeation interplay: supersaturation in an absorptive environment. European Journal of Pharmaceutics and Biopharmaceutics 2012; 82(2):424-428.
11. You X, Xing Q, Tuo J, Song W, Zeng Y, Hu H. Optimizing surfactant content to improve oral bioavailability of ibuprofen in microemulsions: just enough or more than enough? International Journal of Pharmaceutics 2014; 471(1-2):276-284.
12. Singh G, Pai RS. Trans-resveratrol self-nano-emulsifying drug delivery system (SNEDDS) with enhanced bioavailability potential: optimization, pharmacokinetics and in situ single-pass intestinal perfusion (SPIP) studies. Drug Delivery 2015; 22(4):522-530.
13. Ferreira SLC, Bruns RE, Ferreira HS, Matos GD, David JM, Brandão GC, da Silva EGP, Portugal LA, dos Reis PS, Souza AS, dos Santos WLN. Box-Behnken design: an alternative for the optimization of analytical methods. Analytica Chimica Acta 2007; 597(2):179–186.
14. Singh B, Singh R, Bandyopadhyay S, Kapil R, Garg B. Optimized nanoemulsifying systems with enhanced bioavailability of carvedilol. Colloids and Surfaces B: Biointerfaces 2013; 101:465–474.
15. Quinlan PJ, Tanvir A, Tam KC. Application of the central composite design to study the flocculation of an anionic azo dye using quaternized cellulose nanofibrils. Carbohydrate Polymers 2015; 133:80-89.
16. Gupta S, Chavhan S, Sawant KK. Self-nanoemulsifying drug delivery system for adefovir dipivoxil: Design, characterization, in-vitro and ex-vivo evaluation. *Colloids and Surfaces A: Physicochemical and Engineering Aspects* 2011; 392(1):145-155.
17. Date AA, Nagarsenker MS. Design and evaluation of self-nanoemulsifying drug delivery systems (SNEDDS) for cefpodoxime proxetil. International Journal of Pharmaceutics 2007; 329(1-2):166–172.
18. Nazzal S, Khan MA. Response surface methodology for the optimization of ubiquinone self-nanoemulsified drug delivery system. AAPS PharmSciTech 2002; 3(1):E3.
19. Mahmoud H, Al-Suwayeh S, Elkadi S. Design and optimization of self-nano emulsifying drug delivery systems of simvastatin aiming dissolution enhancement. African Journal of Pharmacy and Pharmacology 2013; 7(22):1482-1500.
20. Kallakunta VR, Bandari S, Jukanti R, Veerareddy PR. Oral self-emulsifying powder of lercanidipine hydrochloride: formulation and evaluation. Powder Technology 2012; 221:375–382.
21. Tran TH, Guo Y, Song D, Bruno RS, Lu X. Quercetin-containing self-nano emulsifying drug delivery system for improving oral bioavailability. Journal of Pharmaceutical Sciences 2014; 103(3):840-852.
22. Zhang P, Liu Y, Feng N, Xu J. Preparation and evaluation of self-micro emulsifying drug delivery system of oridonin. International Journal of Pharmaceutics 2008; 355(1-2):269–276.
23. Pouton CW, Porter CJ. Formulation of lipid-based delivery systems for oral administration: materials, methods and strategies. Advanced Drug Delivery Reviews 2008; 60(6):625–637.
24. Kollipara S, Gandhi RK. Pharmacokinetic Aspects and *In Vitro–In Vivo* Correlation Potential for Lipid-Based Formulations. Acta Pharmaceutica Sinica B 2014; 4(3):333–349.
25. Cerpnjak K, Zvonar A, Gasperlin M, Vrecer F. Lipid-Based Systems as a Promising Approach for Enhancing the Bioavailability of Poorly Water-Soluble Drugs. Acta Pharmaceutica 2013; 63(4):427–445.
26. Nepal PR, Han HK, Choi HK. Preparation and *In Vitro-In Vivo* Evaluation ofWitepsol®® H35 Based Self-Nanoemulsifying Drug Delivery Systems (SNEDDS) of Coenzyme Q10. European Journal of Pharmaceutical Sciences 2010; 39(4):224–232.